

Binary black hole spectroscopy: a toupee test of GW190814 and GW190412

Collin D. Capano* and Alexander H. Nitz

Max-Planck-Institut für Gravitationsphysik (Albert-Einstein-Institut), D-30167 Hannover, Germany and
Leibniz Universität Hannover, D-30167 Hannover, Germany

(Dated: August 6, 2020)

Gravitational waves provide a window to probe general relativity (GR) under extreme conditions. The recent observations of GW190412 and GW190814 are unique high-mass-ratio mergers that enable the observation of gravitational-wave harmonics beyond the dominant $\ell = m = 2$ mode. Using these events, we search for physics beyond GR by allowing the source parameters measured from the sub-dominant harmonics to deviate from that of the dominant mode. All results are consistent with GR. We constrain the chirp mass as measured by the $\ell = m = 3$ mode to be within $0^{+6}_{-4}\%$ of the dominant mode when we allow both the masses and spins of the sub-dominant modes to deviate. If we allow only the mass parameters to deviate, we constrain the chirp mass of the $\ell = m = 3$ mode to be within $\pm 1\%$ of the expected value from GR.

I. INTRODUCTION

Advanced LIGO [1] and Virgo [2] have detected more than a dozen binary black hole mergers to date [3–9], with dozens of additional candidates reported during the recently concluded third observing run [10]. The most recent two binary black hole detections, GW190412 [11] and GW190814 [12] were found to have unusually asymmetric masses, with mass ratio ~ 3 and 9 , respectively. High-mass-ratio mergers such as these provide new insights into binary black hole formation channels [13–17]. GW190814, in particular, has sparked considerable interest. Its lighter component object — which had a mass of $\sim 2.6 M_{\odot}$ — is within the hypothesized lower “mass gap” [12, 18–21], challenging existing formation models [22–29].

In addition to providing insights into stellar evolution, the direct detection of binary black holes with gravitational waves has provided new opportunities to test general relativity (GR) in the strong-field regime [30–40]. One of the most exciting (and elusive) possibilities in this new era is a test of the no-hair theorem [41–49]. The no-hair theorem states that all stationary black holes are entirely characterized by three externally observable parameters: the object’s mass, spin, and charge [50, 51]. This is reduced to just mass and spin for astrophysical black holes, as it is difficult for them to accumulate any appreciable charge. A compact object that requires more than two parameters to characterize it is therefore not a black hole as described by GR.

Although the no-hair theorem is a statement about stationary black holes, a perturbed black hole will radiate gravitational waves, thereby asymptoting to a Kerr spacetime. For small perturbations, the emitted gravitational wave is a superposition of quasi-normal modes (QNM) [52–55]. As a consequence of the no-hair theorem, the frequency and damping times of these modes are uniquely defined by the black hole’s mass and spin. This

suggests a test [47]: infer the mass and spin from each mode separately, then compare the estimates. A discrepancy would imply a violation of the no-hair theorem. Several studies have investigated applying this test (known as *black hole spectroscopy*) to the final black hole that is formed after a binary black hole merger [46, 47, 56–61].

Performing black hole spectroscopy on a binary merger remnant is challenging. The post-merger waveform damps away quickly [in $\mathcal{O}(\text{ms})$ for stellar-mass black holes], and the amplitudes of the sub-dominant modes are (at best) $\lesssim 30\%$ of the dominant mode [62]. The signal-to-noise ratio (SNR) of the pertinent signal is therefore relatively small. Furthermore, *when* the post-merger perturbation is sufficiently small such that linear-perturbation theory can be applied is a matter of debate. Many studies have suggested it is necessary to wait at least $10M$ after the merger [30, 63, 64]. However, Giesler et al. [60] argued that the signal immediately after merger can be modelled as a superposition of QNMs if overtones of the dominant mode are included. This substantially increases the SNR available for spectroscopy, but introduces additional technical and conceptual issues that are still being resolved [42, 45, 65, 66]. Even so, the best constraint to date from that approach (obtained on the frequency of the loudest overtone) is only $\sim \pm 40\%$ of the expected GR value (90% credible interval) [44].

In this letter we take a different tack: we perform *binary* black hole spectroscopy. We use the entire observable signal to search for hints of non-GR degrees of freedom, which we generically refer to as “hair”. A similar approach is investigated in Islam et al. [61]. The full gravitational wave can be decomposed into a superposition of spin-weighted spherical harmonics. As with quasi-normal modes, all of the harmonics are functions of the “intrinsic” parameters of the binary. Binary black holes with circular orbits are uniquely defined by eight intrinsic parameters — the two components’ masses and spins. Motivated by traditional black hole spectroscopy, we allow the intrinsic parameters measured by each gravitational-wave mode to independently vary along with an overall phase. In other words, we search for hair in the *full* system, which includes both the initial black holes and the

* collin.capano@aei.mpg.de

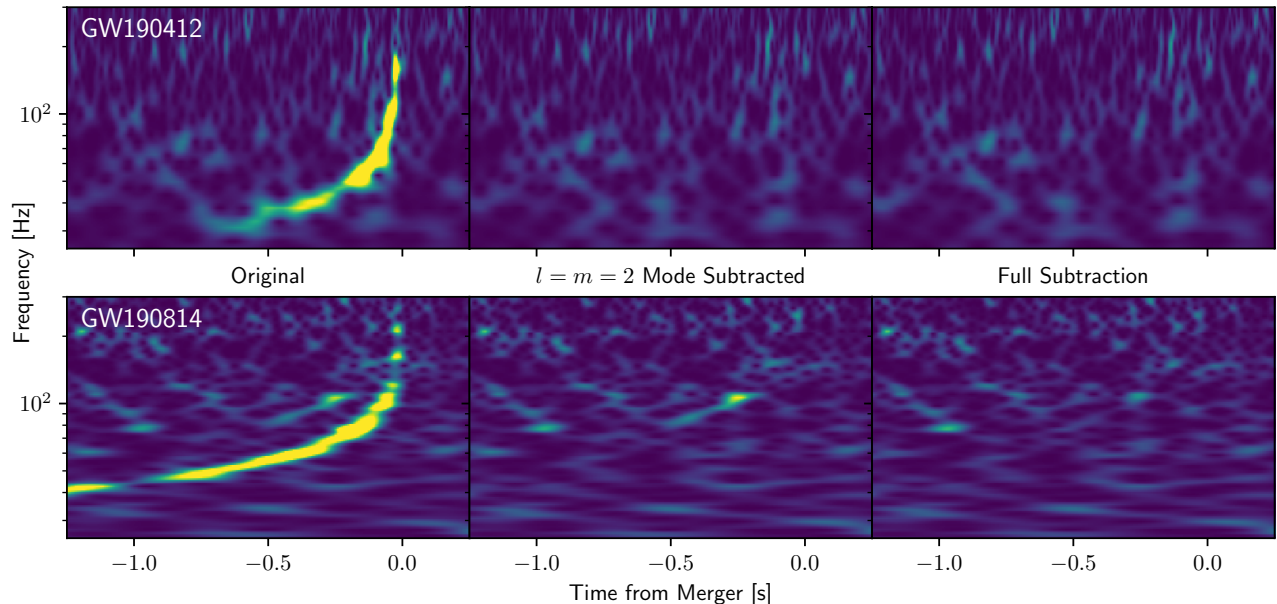


FIG. 1. Time-frequency plot of the coherently-summed data around GW190412 (top) and GW190814 (bottom). The unaltered data (left) is shown along with the residuals after subtracting only the $\ell = m = 2$ mode (center) or the full signal model (right) at the maximum-likelihood parameters. Faint visual evidence of the $\ell = m = 3$ mode is apparent for GW190814, which has $\text{SNR} \sim 7$ and roughly parallels the clear $\ell = m = 2$ mode, but at $1.5\times$ higher frequency.

final black hole.

We apply this method to GW190412 and GW190814. Due to its low mass, uncertainty exists as to whether the lighter object in GW190814 is a neutron star or a black hole [12]. Here, we assume it is a black hole. This is reasonable given that observations of the binary neutron star merger GW170817 disfavor neutron-star equations of state that support masses $\gtrsim 2.3 M_{\odot}$ [67]. Figure 1 shows the data surrounding both of these mergers. With SNRs of 3.5 and 7, respectively, in their $\ell = m = 3$ mode, GW190412 and GW190814 are the only two detections to date that have a measureable sub-dominant mode.

II. BINARY BLACK HOLE SPECTROSCOPY

The full gravitational wave as seen by an external observer at distance D_L from the source can be decomposed into a spin-weighted spherical harmonic basis,

$$h_{(+,\times)} = \frac{1}{D_L} (\Re, \Im) \sum_{\ell m} {}_{-2}Y_{\ell m}(\iota, \phi) A_{\ell m}(\Theta) e^{-i(\Psi_{\ell m}(\Theta) + m\phi_c)}. \quad (1)$$

Here, $h_{(+,\times)}$ is the “plus” and “cross” polarization of the gravitational wave, the inclination ι is the angle between the line-of-sight of the observer and the z -axis of the center-of-mass frame of the source, and ϕ is the azimuthal angle of the observer with respect to this frame. The source frame is oriented such that the z -axis is aligned

with the orbital angular momentum at some fiducial reference time (here, chosen as the time that the frequency of the dominant-mode is 20 Hz); ϕ_c is the phase of the gravitational wave at that time.

The set Θ represents all of the intrinsic parameters describing the source binary. Unless the binary was formed by a recent dynamical capture, the orbit circularizes before it enters the sensitive frequency band of the LIGO and Virgo instruments [68]. Therefore, assuming circular orbits, a binary black hole is uniquely defined by eight parameters: the two component masses $m_{(1,2)}$ and the magnitude and orientation of each object’s spin $\vec{\chi}_{(1,2)}$ at a reference epoch.

To perform spectroscopy on the full waveform, we allow the intrinsic parameters and the phase of the sub-dominant modes to deviate from the dominant, $\ell = m = 2$ mode. In other words, we replace Θ and ϕ_c in Eq. (1) with $\Theta_{\ell m}$ and $\phi_{c,\ell m}$, respectively. We examine two cases. In the first, we allow all intrinsic parameters (masses and spins) of the sub-dominant modes to independently diverge from the dominant mode. In the second scenario we only allow the mass parameters to differ. In both cases we allow ϕ_c to vary.

We expect any deviations from GR, if present, to be small. Since a binary’s chirp mass $\mathcal{M} = (m_1 m_2)^{3/5} / (m_1 + m_2)^{1/5}$ is more accurately measured than the individual component masses, we parameterize the sub-dominant masses in terms of fractional deviations from the dominant-mode chirp mass \mathcal{M}_{22} and symmetric mass ratio $\eta_{22} = m_{1,22} m_{2,22} / (m_{1,22} + m_{2,22})^2$. Specifi-

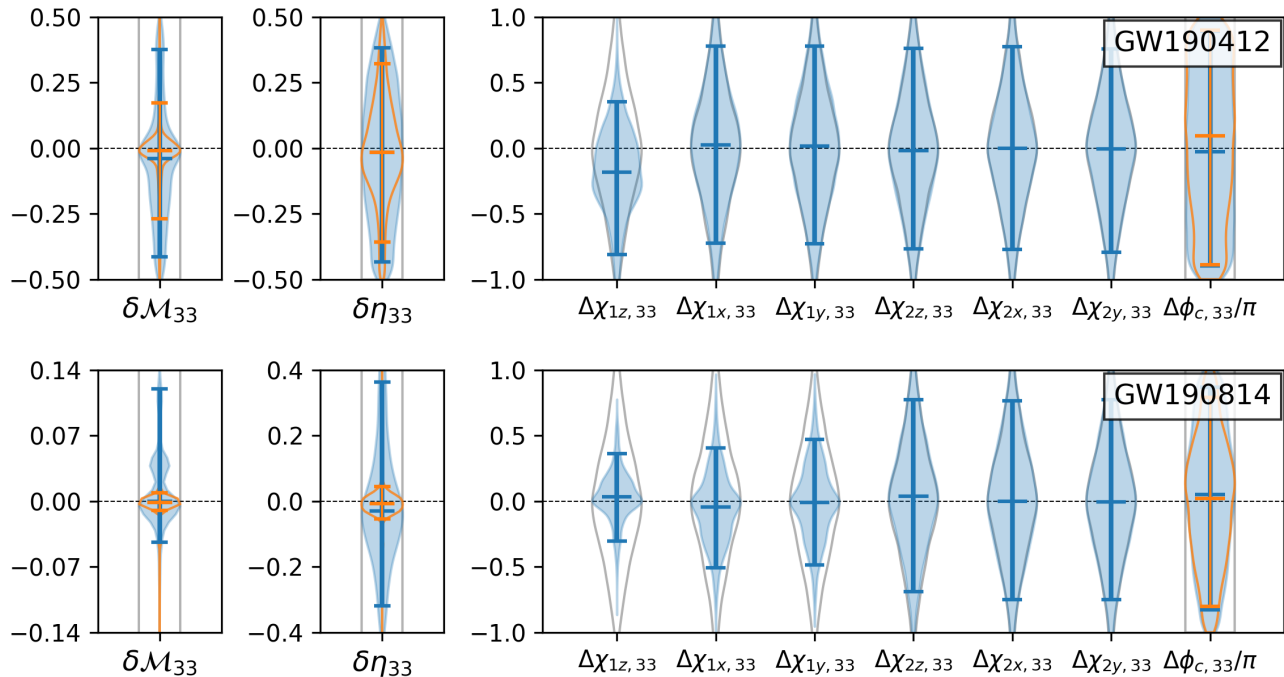


FIG. 2. Marginal posterior distributions of the $\ell m = 33$ deviation parameters for GW190412 (top) and GW190814 (bottom). Blue regions/lines are from the analysis in which we allow both the masses and spins to deviate. Orange lines show the same result when the sub-dominant mode spins are fixed to the dominant-mode value. Horizontal hashes indicate the median (center) and 90% credible regions. Gray lines show the prior distribution.

cally, we define

$$\begin{aligned}\mathcal{M}_{\ell m} &\equiv \mathcal{M}_{22}(1 + \delta\mathcal{M}_{\ell m}), \\ \eta_{\ell m} &\equiv \eta_{22}(1 + \delta\eta_{\ell m}),\end{aligned}$$

and allow $\delta\mathcal{M}_{\ell m}$ and $\delta\eta_{\ell m}$ to vary uniformly between ± 0.5 . The spins are varied independently for each mode, using the same prior (uniform in magnitude and isotropic in direction) as the dominant mode spins. We then report the absolute difference from the dominant mode for each component,

$$\Delta\chi_{ik,\ell m} \equiv \chi_{ik,\ell m} - \chi_{ik,22},$$

where $i = 1, 2$ and $k = x, y, z$. The absolute difference in the modes' phase $\Delta\phi_{c,\ell m} = \phi_{c,\ell m} - \phi_{c,22}$ is varied uniformly between $\pm\pi$. We use standard astrophysical priors for the remaining parameters: uniform distributions are used for comoving volume, coalescence time, phase, and the source-frame component masses $m_{1,2}^{\text{sr}}S$; isotropic distributions are used for sky location, inclination, and polarization.

To model the gravitational-wave signal, we use the recently developed IMRPhenomXPHM waveform [69]. This model includes the effects of both orbital precession and sub-dominant modes on the gravitational waveform, and has been tested against numerical relativity simulations. We model the gravitational wave signals as the sum of the dominant and two sub-dominant modes;

namely, the $\ell = m = 3$ and $\ell = 2, m = 1$ gravitational-wave modes. Other higher modes are neglected in our analysis. To sample the parameter space, we use the open-source PyCBC Inference toolkit [70, 71] with the parallel tempered emcee-based sampler [72, 73].

III. RESULTS

Constraints on the deviations of the $\ell m = 33$ mode for each event are shown in Fig. 2. We report marginalized posterior distributions on the fractional difference in chirp mass $\delta\mathcal{M}_{33}$ and symmetric mass ratio $\delta\eta_{33}$ from the 22 mode, along with the absolute differences in the six spin components and the reference phase ϕ_c . All parameters are consistent with the GR values: a zero deviation is within the 90% credible interval of every parameter.

We obtain the strongest constraints from GW190814, with its $\delta\mathcal{M}_{33}$ being the best constrained parameter overall. We also obtain non-trivial constraints on that event's $\delta\eta_{33}$ and the z -component of the spin of the heavier object, $\Delta\chi_{1z,33}$. All other parameters, including all deviations on the 21 mode (not shown) yield negligible constraints. Using the posterior on $\delta\mathcal{M}_{33}$ and $\delta\eta_{33}$, we reconstruct the masses of the source-frame masses as measured by the 33 mode. The resulting posterior is shown in Fig. 3. Consistent with GR, the posteriors are centered on the values measured by the dominant mode.

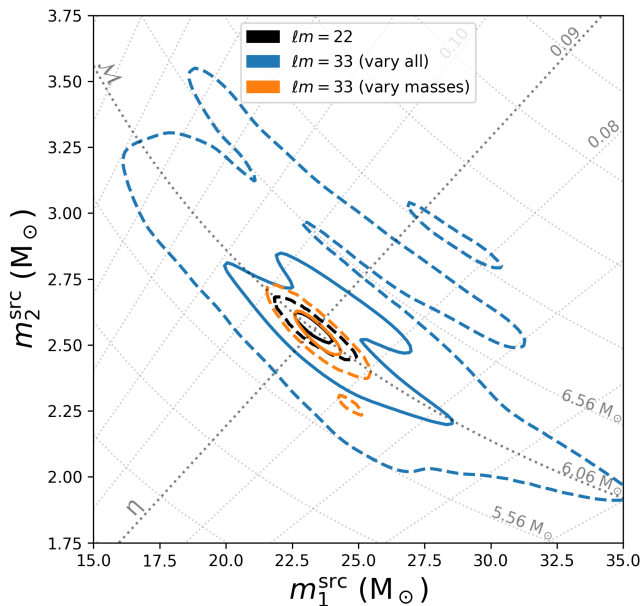


FIG. 3. Marginal posterior distributions on the source-frame component masses $m_{1,2}^{\text{src}}$ of GW190814, as measured by the dominant ($\ell m = 22$) and $\ell m = 33$ modes. The contours show the 50% (solid) and 90% (dashed) credible regions. Lines of constant chirp mass \mathcal{M} and symmetric mass ratio η are indicated by the gray dotted lines, with the darker lines indicating the maximum likelihood value of the 22 mode. Black lines show the posterior on the masses as measured by the 22 mode, blue lines show the 33 mode when spins are allowed to deviate along with the masses and phase; orange lines show the 33 mode when only the masses and phase are allowed to deviate.

Under the assumption that the mass deviation parameters, $\delta\mathcal{M}_{33}$ and $\delta\eta_{33}$, are common between GW190412 and GW190814, we resample their likelihoods using a kernel density estimate and obtain the joint constraints shown in Fig. 4. A full summary of our analyses’ marginalized constraints are shown in Table I.

IV. DISCUSSION

We developed a test to look for physics beyond general relativity by using the harmonic information from binary black hole mergers. We found no evidence for a violation of general relativity. This test has been enabled by the recent detection of high-mass-ratio mergers by Advanced LIGO and Virgo. Over the next few years, as the detectors reach design sensitivity, we expect the rate of mergers to increase by a factor of 5–10 [74]. This should improve the limits observed here by a factor of ~ 2 –3, or more, if even larger mass-ratio mergers are observed.

The question arises, what exactly are we testing? Performing spectroscopy on the full gravitational waveform introduces conceptual issues not present in standard black hole spectroscopy. Unlike the final object, which is

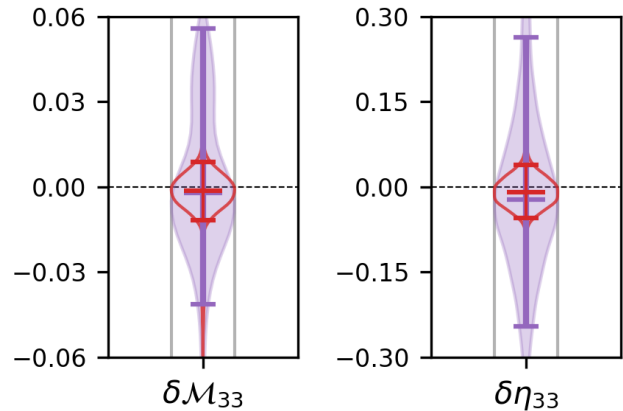


FIG. 4. Combined marginal posterior distributions of $\delta\mathcal{M}_{33}$ and $\delta\eta_{33}$ from GW190412 and GW190814. Purple regions/lines are from the analysis in which we allow both the masses and spins to deviate. Red lines show the same result when we fix the sub-dominant mode spins to the dominant-mode value. Horizontal hashes indicate the median (center) and 90% credible regions. Gray lines show the prior distribution.

Event	Analysis	$\delta\mathcal{M}_{33}$ (%)	$\delta\eta_{33}$ (%)	$\Delta\chi_{1z,33}$
GW190412	all	-4^{+41}_{-38}	-2^{+40}_{-42}	$-0.18^{+0.54}_{-0.63}$
	masses	-1^{+18}_{-26}	-2^{+34}_{-34}	–
GW190814	all	0^{+12}_{-4}	-3^{+39}_{-29}	$0.03^{+0.33}_{-0.34}$
	masses	0^{+1}_{-1}	-1^{+5}_{-5}	–
Combined	all	0^{+6}_{-4}	-2^{+29}_{-22}	–
	masses	0^{+1}_{-1}	-1^{+5}_{-5}	–

TABLE I. Median and 90% credible intervals on deviations of the $\ell = m = 3$ chirp mass $\delta\mathcal{M}_{33}$, symmetric-mass ratio $\delta\eta_{33}$, and (where applicable) the z -component of the heavier object’s spin $\Delta\chi_{1z,33}$. These are the best-constrained deviation parameters in our analysis; other parameters are weakly constrained. We performed two analyses — one in which the masses, orbital phase, and spins of the sub-dominant modes are allowed to deviate from the dominant mode (“all”) and one in which only the masses and phase are allowed to deviate (“masses”). Constraints on the mass parameters are combined between the two events (“Combined”).

assumed to asymptotically settle into a Kerr black hole, the initial objects are dynamical and never actually Kerr. They are formed a finite amount of time before merger and at a finite distance from each other. Although approximately Kerr when far apart, the objects’ mutual presence causes subtle perturbations in spacetime that are never truly radiated away until the formation of the final black hole. A full description of this residual hair would require knowledge of both objects’ entire history, including the structure and distribution of their stellar matter when they collapsed. That, clearly, is not encapsulated in the nine parameters described above.

However, traditional black hole spectroscopy has its own attendant uncertainties. The final black hole exists in a universe containing other matter. It is therefore never truly a Kerr black hole either, only approximately so. Furthermore, residual non-linearities may exist in the post-merger spacetime that are not captured by the QNM description of the final black hole. While these non-linearities dampen away quickly, the ambiguity over the timescale at which this occurs is a potential source of unaccounted for hair. In other words, both standard black hole spectroscopy and the binary black hole spectroscopy we perform here are subject to modelling systematics.

Black hole spectroscopy may be subject to fewer uncertainties and complexities than binary black hole spectroscopy, but this is more a difference of degree than substance. If hair were detected by one of these tests (in the form of a non-zero deviation parameter), it does not necessarily mean that the objects violate GR. Any number of more mundane effects — modelling uncertainties, wrong assumptions, even unexpected noise features in the detector data — may offer an explanation. As such, these tests are perhaps better described as “toupee tests” rather than no-hair theorem tests. They may detect hair, but whether or not that indicates a violation

of GR (real hair) or other systematics (fake hair) would require further study. Our hope, both with binary black hole spectroscopy and standard black hole spectroscopy, is that these tests may one day detect hair that cannot be explained by more mundane effects. Such a discovery could point the way to new physics.

ACKNOWLEDGMENTS

We acknowledge the Max Planck Gesellschaft. We are extremely grateful to Carsten Aulbert, Henning Fehrmann, and the computing team from AEI Hannover for their significant technical support. We thank Sebastian Khan and Frank Ohme for useful discussions with regards to gravitational-waveform models. This research has made use of data from the Gravitational Wave Open Science Center (<https://www.gw-openscience.org>), a service of LIGO Laboratory, the LIGO Scientific Collaboration and the Virgo Collaboration. LIGO is funded by the U.S. National Science Foundation. Virgo is funded by the French Centre National de Recherche Scientifique (CNRS), the Italian Istituto Nazionale della Fisica Nucleare (INFN) and the Dutch Nikhef, with contributions by Polish and Hungarian institutes.

-
- [1] J. Aasi *et al.* (LIGO Scientific Collaboration), Advanced LIGO, *Class. Quantum Grav.* **32**, 074001 (2015), [arXiv:1411.4547 \[gr-qc\]](https://arxiv.org/abs/1411.4547).
 - [2] F. Acernese *et al.* (VIRGO), Advanced Virgo: a second-generation interferometric gravitational wave detector, *Class. Quantum Grav.* **32**, 024001 (2015), [arXiv:1408.3978 \[gr-qc\]](https://arxiv.org/abs/1408.3978).
 - [3] A. H. Nitz, C. Capano, A. B. Nielsen, S. Reyes, R. White, D. A. Brown, and B. Krishnan, 1-OGC: The first open gravitational-wave catalog of binary mergers from analysis of public Advanced LIGO data, *Astrophys. J.* **872**, 195 (2019), [arXiv:1811.01921 \[gr-qc\]](https://arxiv.org/abs/1811.01921).
 - [4] A. H. Nitz, T. Dent, G. S. Davies, S. Kumar, C. D. Capano, I. Harry, S. Mozzon, L. Nuttall, A. Lundgren, and M. Tápai, 2-OGC: Open Gravitational-wave Catalog of binary mergers from analysis of public Advanced LIGO and Virgo data, *Astrophys. J.* **891**, 123 (2019), [arXiv:1910.05331 \[astro-ph.HE\]](https://arxiv.org/abs/1910.05331).
 - [5] A. H. Nitz, T. Dent, G. S. Davies, and I. Harry, A search for gravitational waves from binary mergers with a single observatory, *The Astrophysical Journal* **897**, 169 (2020).
 - [6] T. Venumadhav, B. Zackay, J. Roulet, L. Dai, and M. Zaldarriaga, New search pipeline for compact binary mergers: Results for binary black holes in the first observing run of Advanced LIGO, *Phys. Rev. D* **100**, 023011 (2019), [arXiv:1902.10341 \[astro-ph.IM\]](https://arxiv.org/abs/1902.10341).
 - [7] T. Venumadhav, B. Zackay, J. Roulet, L. Dai, and M. Zaldarriaga, New binary black hole mergers in the second observing run of Advanced LIGO and Advanced Virgo, *Phys. Rev. D* **101**, 083030 (2020), [arXiv:1904.07214 \[astro-ph.HE\]](https://arxiv.org/abs/1904.07214).
 - [8] B. Zackay, L. Dai, T. Venumadhav, J. Roulet, and M. Zaldarriaga, Detecting Gravitational Waves With Disparate Detector Responses: Two New Binary Black Hole Mergers, (2019), [arXiv:1910.09528 \[astro-ph.HE\]](https://arxiv.org/abs/1910.09528).
 - [9] B. P. Abbott *et al.* (LIGO Scientific, Virgo), GWTC-1: A Gravitational-Wave Transient Catalog of Compact Binary Mergers Observed by LIGO and Virgo during the First and Second Observing Runs, *Phys. Rev. X* **9**, 031040 (2019), [arXiv:1811.12907 \[astro-ph.HE\]](https://arxiv.org/abs/1811.12907).
 - [10] LVC, [Gracedb — gravitational-wave candidate event database](https://www.lvc.ligo.org/).
 - [11] R. Abbott *et al.* (LIGO Scientific, Virgo), GW190412: Observation of a Binary-Black-Hole Coalescence with Asymmetric Masses, (2020), [arXiv:2004.08342 \[astro-ph.HE\]](https://arxiv.org/abs/2004.08342).
 - [12] R. Abbott *et al.* (LIGO Scientific, Virgo), GW190814: Gravitational Waves from the Coalescence of a 23 Solar Mass Black Hole with a 2.6 Solar Mass Compact Object, *Astrophys. J.* **896**, L44 (2020), [arXiv:2006.12611 \[astro-ph.HE\]](https://arxiv.org/abs/2006.12611).
 - [13] A. Olejak, M. Fishbach, K. Belczynski, D. Holz, J.-P. Lasota, M. Miller, and T. Bulik, The Origin of inequality: isolated formation of a 30+10Msun binary black-hole merger, (2020), [arXiv:2004.11866 \[astro-ph.HE\]](https://arxiv.org/abs/2004.11866).
 - [14] C. L. Rodriguez *et al.*, GW190412 as a Third-Generation Black Hole Merger from a Super Star Cluster, *Astrophys. J.* **896**, L10 (2020), [arXiv:2005.04239 \[astro-ph.HE\]](https://arxiv.org/abs/2005.04239).
 - [15] A. S. Hamers and M. Safarzadeh, Was GW190412 born from a hierarchical 3+1 quadruple configuration?, (2020), [arXiv:2005.03045 \[astro-ph.HE\]](https://arxiv.org/abs/2005.03045).
 - [16] D. Gerosa, S. Vitale, and E. Berti, Astrophysical implications of GW190412 as a remnant of a previous black-hole

- merger, (2020), [arXiv:2005.04243 \[astro-ph.HE\]](#).
- [17] M. Safarzadeh and K. Hotokezaka, Being careful with field formation interpretation of GW190412, *Astrophys. J.* **897**, L7 (2020), [arXiv:2005.06519 \[astro-ph.HE\]](#).
- [18] W. M. Farr, N. Sravan, A. Cantrell, L. Kreidberg, C. D. Bailyn, *et al.*, The Mass Distribution of Stellar-Mass Black Holes, *Astrophys. J.* **741**, 103 (2011), [arXiv:1011.1459 \[astro-ph.GA\]](#).
- [19] C. D. Bailyn, R. K. Jain, P. Coppi, and J. A. Orosz, The mass distribution of stellar black holes, *The Astrophysical Journal* **499**, 367 (1998).
- [20] F. Ozel, D. Psaltis, R. Narayan, and J. E. McClintock, The Black Hole Mass Distribution in the Galaxy, *Astrophys. J.* **725**, 1918 (2010), [arXiv:1006.2834 \[astro-ph.GA\]](#).
- [21] F. Ozel, D. Psaltis, R. Narayan, and A. S. Villarreal, On the Mass Distribution and Birth Masses of Neutron Stars, *Astrophys. J.* **757**, 55 (2012), [arXiv:1201.1006 \[astro-ph.HE\]](#).
- [22] M. Zevin, M. Spera, C. P. Berry, and V. Kalogera, Exploring the Lower Mass Gap and Unequal Mass Regime in Compact Binary Evolution, (2020), [arXiv:2006.14573 \[astro-ph.HE\]](#).
- [23] T. Broadhurst, J. M. Diego, and G. F. Smoot, Interpreting LIGO/Virgo "Mass-Gap" events as lensed Neutron Star-Black Hole binaries, (2020), [arXiv:2006.13219 \[astro-ph.CO\]](#).
- [24] M. Safarzadeh and A. Loeb, Formation of mass-gap objects in highly asymmetric mergers, (2020), [arXiv:2007.00847 \[astro-ph.HE\]](#).
- [25] N.-B. Zhang and B.-A. Li, GW190814's secondary component with mass $(2.50 - 2.67) M_{\odot}$ as a super-fast pulsar, (2020), [arXiv:2007.02513 \[astro-ph.HE\]](#).
- [26] I. Mandel, B. Mueller, J. Riley, S. E. de Mink, A. Vigna-Gomez, and D. Chattopadhyay, Binary population synthesis with probabilistic remnant mass and kick prescriptions, (2020), [arXiv:2007.03890 \[astro-ph.HE\]](#).
- [27] Y. Yang, V. Gayathri, I. Bartos, Z. Haiman, M. Safarzadeh, and H. Tagawa, Black Hole Formation in the Lower Mass Gap through Mergers and Accretion in AGN Disks, (2020), [arXiv:2007.04781 \[astro-ph.HE\]](#).
- [28] D. A. Godzieba, D. Radice, and S. Bernuzzi, On the maximum mass of neutron stars and GW190814, (2020), [arXiv:2007.10999 \[astro-ph.HE\]](#).
- [29] V. Dexheimer, R. Gomes, T. Klöhn, S. Han, and M. Salinas, GW190814 as a massive rapidly-rotating neutron star with exotic degrees of freedom, (2020), [arXiv:2007.08493 \[astro-ph.HE\]](#).
- [30] B. Abbott *et al.* (LIGO Scientific, Virgo), Tests of general relativity with GW150914, *Phys. Rev. Lett.* **116**, 221101 (2016), [Erratum: *Phys. Rev. Lett.* 121, 129902 (2018)], [arXiv:1602.03841 \[gr-qc\]](#).
- [31] N. Krishnendu, M. Saleem, A. Samajdar, K. Arun, W. Del Pozzo, and C. K. Mishra, Constraints on the binary black hole nature of GW151226 and GW170608 from the measurement of spin-induced quadrupole moments, *Phys. Rev. D* **100**, 104019 (2019), [arXiv:1908.02247 \[gr-qc\]](#).
- [32] Y.-F. Wang, R. Niu, T. Zhu, and W. Zhao, Gravitational-Wave Implications for the Parity Symmetry of Gravity at GeV Scale, (2020), [arXiv:2002.05668 \[gr-qc\]](#).
- [33] B. P. Abbott *et al.* (VIRGO, LIGO Scientific), GW170104: Observation of a 50-Solar-Mass Binary Black Hole Coalescence at Redshift 0.2, *Phys. Rev. Lett.* **118**, 221101 (2017), [Erratum: *Phys. Rev. Lett.* 121, no. 12, 129901 (2018)], [arXiv:1706.01812 \[gr-qc\]](#).
- [34] B. Abbott *et al.* (LIGO Scientific, Virgo), Tests of General Relativity with the Binary Black Hole Signals from the LIGO-Virgo Catalog GWTC-1, *Phys. Rev. D* **100**, 104036 (2019), [arXiv:1903.04467 \[gr-qc\]](#).
- [35] A. Nielsen and O. Birnholz, Gravitational wave bounds on dirty black holes, *Astron. Nachr.* **340**, 116 (2019).
- [36] G. Carullo, G. Riemenschneider, K. W. Tsang, A. Nagar, and W. Del Pozzo, GW150914 peak frequency: a novel consistency test of strong-field General Relativity, *Class. Quant. Grav.* **36**, 105009 (2019), [arXiv:1811.08744 \[gr-qc\]](#).
- [37] C.-J. Haster, Pi from the sky – A null test of general relativity from a population of gravitational wave observations, (2020), [arXiv:2005.05472 \[gr-qc\]](#).
- [38] X. Liu, V. F. He, T. M. Mikulski, D. Palenova, C. E. Williams, J. Creighton, and J. D. Tasson, Measuring the speed of gravitational waves from the first and second observing run of Advanced LIGO and Advanced Virgo, *Phys. Rev. D* **102**, 024028 (2020), [arXiv:2005.03121 \[gr-qc\]](#).
- [39] L. Shao, Combined search for anisotropic birefringence in the gravitational-wave transient catalog GWTC-1, *Phys. Rev. D* **101**, 104019 (2020), [arXiv:2002.01185 \[hep-ph\]](#).
- [40] M. Cabero, C. D. Capano, O. Fischer-Birnholtz, B. Krishnan, A. B. Nielsen, A. H. Nitz, and C. M. Biwer, Observational tests of the black hole area increase law, *Phys. Rev. D* **97**, 124069 (2018), [arXiv:1711.09073 \[gr-qc\]](#).
- [41] I. Ota and C. Chirenti, Overtones or higher harmonics? Prospects for testing the no-hair theorem with gravitational wave detections, *Phys. Rev. D* **101**, 104005 (2020), [arXiv:1911.00440 \[gr-qc\]](#).
- [42] X. J. Forteza, S. Bhagwat, P. Pani, and V. Ferrari, On the spectroscopy of binary black hole ringdown using overtones and angular modes, (2020), [arXiv:2005.03260 \[gr-qc\]](#).
- [43] A. Maselli, K. Kokkotas, and P. Laguna, Observing binary black hole ringdowns by advanced gravitational wave detectors, *Phys. Rev. D* **95**, 104026 (2017), [arXiv:1702.01110 \[gr-qc\]](#).
- [44] M. Isi, M. Giesler, W. M. Farr, M. A. Scheel, and S. A. Teukolsky, Testing the no-hair theorem with GW150914, *Phys. Rev. Lett.* **123**, 111102 (2019), [arXiv:1905.00869 \[gr-qc\]](#).
- [45] S. Bhagwat, X. J. Forteza, P. Pani, and V. Ferrari, Ringdown overtones, black hole spectroscopy, and no-hair theorem tests, *Phys. Rev. D* **101**, 044033 (2020), [arXiv:1910.08708 \[gr-qc\]](#).
- [46] M. Cabero, J. Westerweck, C. D. Capano, S. Kumar, A. B. Nielsen, and B. Krishnan, Black hole spectroscopy in the next decade, *Phys. Rev. D* **101**, 064044 (2020), [arXiv:1911.01361 \[gr-qc\]](#).
- [47] O. Dreyer, B. J. Kelly, B. Krishnan, L. S. Finn, D. Garrison, and R. Lopez-Aleman, Black hole spectroscopy: Testing general relativity through gravitational wave observations, *Class. Quant. Grav.* **21**, 787 (2004), [arXiv:gr-qc/0309007](#).
- [48] A. Maselli, P. Pani, L. Gualtieri, and E. Berti, Parametrized ringdown spin expansion coefficients: a data-analysis framework for black-hole spectroscopy with multiple events, *Phys. Rev. D* **101**, 024043 (2020), [arXiv:1910.12893 \[gr-qc\]](#).

- [49] S. Bhagwat, M. Cabero, C. D. Capano, B. Krishnan, and D. A. Brown, Detectability of the subdominant mode in a binary black hole ringdown, *Phys. Rev. D* **102**, 024023 (2020), [arXiv:1910.13203 \[gr-qc\]](#).
- [50] B. Carter, Axisymmetric black hole has only two degrees of freedom, *Phys. Rev. Lett.* **26**, 331 (1971).
- [51] W. Israel, Event horizons in static vacuum space-times, *Phys. Rev.* **164**, 1776 (1967).
- [52] C. V. Vishveshwara, Scattering of Gravitational Radiation by a Schwarzschild Black-hole, *Nature* **227**, 936 (1970).
- [53] W. H. Press, Long Wave Trains of Gravitational Waves from a Vibrating Black Hole, *Astrophys. J. Lett.* **170**, L105 (1971).
- [54] S. A. Teukolsky, Perturbations of a rotating black hole. 1. Fundamental equations for gravitational electromagnetic and neutrino field perturbations, *Astrophys. J.* **185**, 635 (1973).
- [55] S. Chandrasekhar and S. L. Detweiler, The quasi-normal modes of the Schwarzschild black hole, *Proc. Roy. Soc. Lond.* **A344**, 441 (1975).
- [56] E. Berti, V. Cardoso, and C. M. Will, On gravitational-wave spectroscopy of massive black holes with the space interferometer LISA, *Phys. Rev. D* **73**, 064030 (2006), [arXiv:gr-qc/0512160](#).
- [57] E. Berti, J. Cardoso, V. Cardoso, and M. Cavaglia, Matched-filtering and parameter estimation of ringdown waveforms, *Phys. Rev. D* **76**, 104044 (2007), [arXiv:0707.1202 \[gr-qc\]](#).
- [58] S. Gossan, J. Veitch, and B. Sathyaprakash, Bayesian model selection for testing the no-hair theorem with black hole ringdowns, *Phys. Rev. D* **85**, 124056 (2012), [arXiv:1111.5819 \[gr-qc\]](#).
- [59] E. Berti, A. Sesana, E. Barausse, V. Cardoso, and K. Belczynski, Spectroscopy of Kerr black holes with Earth- and space-based interferometers, *Phys. Rev. Lett.* **117**, 101102 (2016), [arXiv:1605.09286 \[gr-qc\]](#).
- [60] M. Giesler, M. Isi, M. A. Scheel, and S. Teukolsky, Black Hole Ringdown: The Importance of Overtones, *Phys. Rev. X* **9**, 041060 (2019), [arXiv:1903.08284 \[gr-qc\]](#).
- [61] T. Islam, A. K. Mehta, A. Ghosh, V. Varma, P. Ajith, and B. Sathyaprakash, Testing the no-hair nature of binary black holes using the consistency of multipolar gravitational radiation, *Phys. Rev. D* **101**, 024032 (2020), [arXiv:1910.14259 \[gr-qc\]](#).
- [62] S. Borhanian, K. Arun, H. P. Pfeiffer, and B. Sathyaprakash, Comparison of post-Newtonian mode amplitudes with numerical relativity simulations of binary black holes, *Class. Quant. Grav.* **37**, 065006 (2020), [arXiv:1901.08516 \[gr-qc\]](#).
- [63] A. Buonanno, G. B. Cook, and F. Pretorius, Inspiral, merger and ring-down of equal-mass black-hole binaries, *Phys. Rev. D* **75**, 124018 (2007).
- [64] S. Bhagwat, M. Okounkova, S. W. Ballmer, D. A. Brown, M. Giesler, M. A. Scheel, and S. A. Teukolsky, On choosing the start time of binary black hole ringdowns, *Phys. Rev. D* **97**, 104065 (2018), [arXiv:1711.00926 \[gr-qc\]](#).
- [65] M. Okounkova, Revisiting non-linearity in binary black hole mergers, (2020), [arXiv:2004.00671 \[gr-qc\]](#).
- [66] D. Pook-Kolb, O. Birnholtz, J. L. Jaramillo, B. Krishnan, and E. Schnetter, Horizons in a binary black hole merger II: Fluxes, multipole moments and stability, (2020), [arXiv:2006.03940 \[gr-qc\]](#).
- [67] M. Shibata, E. Zhou, K. Kiuchi, and S. Fujibayashi, Constraint on the maximum mass of neutron stars using GW170817 event, *Phys. Rev. D* **100**, 023015 (2019), [arXiv:1905.03656 \[astro-ph.HE\]](#).
- [68] P. C. Peters, Gravitational Radiation and the Motion of Two Point Masses, *Phys. Rev.* **136**, B1224 (1964).
- [69] G. Pratten *et al.*, Let's twist again: computationally efficient models for the dominant and sub-dominant harmonic modes of precessing binary black holes, (2020), [arXiv:2004.06503 \[gr-qc\]](#).
- [70] C. M. Biwer, C. D. Capano, S. De, M. Cabero, D. A. Brown, A. H. Nitz, and V. Raymond, PyCBC Inference: A Python-based parameter estimation toolkit for compact binary coalescence signals, *Publ. Astron. Soc. Pac.* **131**, 024503 (2019), [arXiv:1807.10312 \[astro-ph.IM\]](#).
- [71] A. H. Nitz, I. W. Harry, J. L. Willis, C. M. Biwer, D. A. Brown, L. P. Pekowsky, T. Dal Canton, A. R. Williamson, T. Dent, C. D. Capano, T. J. Massinger, A. K. Lenon, A. B. Nielsen, and M. Cabero, PyCBC Software, <https://github.com/gwastro/pycbc> (2018).
- [72] W. D. Vousden, W. M. Farr, and I. Mandel, Dynamic temperature selection for parallel tempering in Markov chain Monte Carlo simulations, *Monthly Notices of the Royal Astronomical Society* **455**, 1919 (2015), <https://academic.oup.com/mnras/article-pdf/455/2/1919/18514064/stv2422.pdf>.
- [73] D. Foreman-Mackey, D. W. Hogg, D. Lang, and J. Goodman, emcee: The MCMC Hammer, *Publ. Astron. Soc. Pac.* **125**, 306 (2013), [arXiv:1202.3665 \[astro-ph.IM\]](#).
- [74] B. P. Abbott *et al.* (KAGRA, LIGO Scientific, VIRGO), Prospects for Observing and Localizing Gravitational-Wave Transients with Advanced LIGO, Advanced Virgo and KAGRA, *Living Rev. Rel.* **21**, 3 (2018), [arXiv:1304.0670 \[gr-qc\]](#).